Liouvillian skin effect in a one-dimensional open many-body quantum system with generalized boundary conditions

Liang Mao,[1] Xuanpu Yang,[2] Ming-Jie Tao,[3,*] Haiping Hu,[4,5,†] and Lei Pan[2,‡]

[1]*Institute for Advanced Study, Tsinghua University, Beijing 100084, China*

[2]*School of Physics, Nankai University, Tianjin 300071, China*

[3]*College of Mathematics and Physics, Chengdu University of Technology, Chengdu 610059, China*

[4]*Beijing National Laboratory for Condensed Matter Physics, Institute of Physics, Chinese Academy of Sciences, Beijing 100190, China*

[5]*School of Physical Sciences, University of Chinese Academy of Sciences, Beijing 100049, China*

(Received 5 February 2024; accepted 8 July 2024; published 25 July 2024)

The non-Hermitian skin effect, in which eigenstates of non-Hermitian Hamiltonians are localized at one boundary in the open boundary condition, has attracted great interest recently. In this paper, we investigate the skin effect in one-dimensional dissipative quantum many-body systems, which we call the Liouvillian skin effect (LSE). We rigorously identify the existence of the LSE for generalized boundary conditions by solving the Liouvillian superoperator of an exactly solvable model with the advantage of the Bethe ansatz. The LSE is sensitive to boundary conditions where the signature is reflected in eigenfunctions of the system. We confirm that the LSE is fragile to a tiny coflow boundary hopping with non-Hermitian current but can survive a counterflow boundary hopping in the thermodynamic limit. Our work provides a prototypical example of exactly solvable dissipative quantum many-body lattice systems exhibiting the LSE for generalized boundary conditions. It can be further extended to other integrable open quantum many-body models.

DOI: 10.1103/PhysRevB.110.045440

I. INTRODUCTION

Open systems are ubiquitous, covering the atomic realm to the observable universe. In recent years, open quantum many-body physics has become an important area [1–3], principally due to experimental advances in accurately controlling dissipation and interactions between particles [4–15], and has received considerable theoretical attention [16–78]. Furthermore, recent theoretical progress has revealed that many rich phenomena can emerge from the interplay between dissipations and interparticle interactions, including, but not limited to, parity-time symmetric quantum criticality [16,17], anomalous nonexponential dynamics [24] and non-Hermitian many-body localization [56–60], and negative central charge at an exceptional point [74,75].

A quantum system coupled to environment degrees of freedom constitutes an open quantum system whose time evolution is described by a Lindblad master equation under the Markovian approximation. The dynamics of an open quantum system are dominated by the Liouvillian superoperator and can be described by the effective non-Hermitian Hamiltonian under some circumstances. It has been shown that the non-Hermitian Hamiltonian exhibits unique features, among which the non-Hermitian skin effect (NHSE) [79–83] has attracted growing attention both theoretically [84–107] and experimentally [108–116]. The NHSE states that the eigenstates of a non-Hermitian Hamiltonian can be localized at the boundaries under open boundary conditions, although they remain extended under the periodic boundary condition. This effect originates from the sensitivity of related non-Hermitian terms in the Hamiltonian to boundary perturbations and manifests in not only eigenstates properties but also distinct features of eigenvalues under different boundary conditions.

Previous investigations primarily dealt with the NHSE at the level of single-particle systems and revealed that the NHSE has a dramatic influence on the topology and dynamics. Recently, a number of studies have examined the NHSE in the framework of many-body systems [117–133] and found that the interplay between the NHSE and interaction can give rise to the impact on properties such as the slowdown of relaxation dynamics [117], many-body localization [128], and entanglement transition [129–131]. More recently, the skin effect was identified to exist in the Liouvillian superoperator due to its intrinsic non-Hermiticity and was named the Liouvillian skin effect (LSE) [134–137]. Meanwhile, research on exactly solvable models of open quantum many-body systems gradually has increased, leading to the structure of the Liouvillian in the framework of Yang-Baxter integrability being an emerging field of mathematical physics [138–149].

In the literature, Guo *et al.* [85] demonstrated the existence condition of the NHSE for more general boundary conditions at the single-particle level. Moreover, a recent study [149] revealed that boundary conditions have a significant influence on the integrability of non-Hermitian systems. It is natural to begin investigating the existence of and reveal the connection between the LSE and boundary conditions at the level of

*Contact author: mjt@iphy.ac.cn

†Contact author: hhu@iphy.ac.cn

‡Contact author: panlei@nankai.edu.cn

many-body physics. In this paper, we explore the relationship between the LSE and different boundary conditions using techniques to solve the Liouvillian superoperators that were developed recently. By constructing an exactly solvable Liouvillian superoperator, we find the exact solutions for more general boundary conditions, allowing us to unearth evidence for the existence of the LSE. We find that the LSE is destroyed by a certain type of boundary perturbation but is immune to another type of perturbation. Our work provides firm ground for the existence of the LSE and its sensitivity to boundary effects from the exactly solvable many-body system perspective.

The rest of this paper is organized as follows. In Sec. II, we introduce an exactly solvable Liouvillian superoperator that can be mapped to a non-Hermitian XXZ chain in the subspace. Section III solves the exact solution in the periodic boundary condition (PBC) and the open boundary condition (OBC). Then, we discuss the general boundary condition and identify the existence condition of the LSE in Sec. IV. Finally, we summarize in Sec. V. All the calculation details are provided in the Appendixes.

II. THE MODEL

The time evolution of the density matrix $\rho(t)$ for a Markovian open quantum system is generally governed by the Lindblad master equation [150,151] ($\hbar = 1$),

$$\frac{d\rho(t)}{dt} \equiv \hat{\mathscr{L}}\rho(t) = -i[\hat{H}_S, \rho(t)] + \mathcal{D}[\rho(t)], \tag{1}$$

where $\hat{\mathscr{L}}$ is the Liouvillian superoperator. The first term corresponds to the coherent evolution, and the second term $\mathcal{D}[\rho(t)] = \sum_k [2\hat{L}_k\rho(t)\hat{L}_k^\dagger - \{\hat{\rho}(t), \hat{L}_k^\dagger\hat{L}_k\}]$ gives the dissipation process. Here $[\cdot,\cdot]$ and $\{\cdot,\cdot\}$ denote commutator and anticommutator, respectively. According to the Choi-Jamiołkowski isomorphism [152,153], the Lindblad equation can be expressed as the equivalent equation $\frac{d}{dt}|\rho\rangle = \hat{\mathscr{L}}|\rho\rangle$ with the vectorized density matrix $|\rho\rangle = \sum_{i,j}\rho_{i,j}|i\rangle \otimes |j\rangle$ in double space $\mathcal{H}_R \otimes \mathcal{H}_L$, and the Liouvillian superoperator is written as

$$\begin{aligned}\hat{\mathscr{L}} =& -i\big(\hat{H}_S \otimes \hat{I} - \hat{I} \otimes \hat{H}_S^{\mathrm{T}}\big) \\ &+ \sum_k [2\hat{L}_k \otimes \hat{L}_k^* - \hat{L}_k^\dagger\hat{L}_k \otimes \hat{I} - \hat{I} \otimes (\hat{L}_k^\dagger\hat{L}_k)^{\mathrm{T}}].\end{aligned} \tag{2}$$

The Lindblad equation is determined by the spectrum of $\hat{\mathscr{L}}$. The system reaches a steady state which is the zero-energy eigenstate of $\hat{\mathscr{L}}$. The solvability of $\hat{\mathscr{L}}$ clearly involves the choice of operators $\hat{L}_k$. Typically, the Liouvillian superoperator is not integrable except in special circumstances; for example, $\hat{L}_k$ is chosen to be the single creation and annihilation operator, and the Hamiltonian $\hat{H}_S$ is simply the integrable model. Reference [140] found an alternative mechanism connecting the Lindblad superoperator to known integrable models. Suppose local projectors $\hat{\mathcal{P}}_j^m$ acting on the double space which satisfy $\hat{\mathcal{P}}_j^m\hat{\mathcal{P}}_j^n = \delta_{m,n}\hat{\mathcal{P}}_j^m$ and $\hat{\mathcal{P}}_j^0 = 1 - \sum_m \hat{\mathcal{P}}_j^m$ exist. If all projectors commute with $\hat{\mathscr{L}}$, i.e., $[\hat{\mathscr{L}}, \hat{\mathcal{P}}_j^m] = 0$, then the double space can be decomposed by a series of subspaces which are the eigenspace of projector set $\{\hat{P}_j^m\}$. These subspaces are invariant spaces of the Liouvillian superoperator. If we choose the dissipation operator $\hat{L}_k$ and Hamiltonian $\hat{H}_S$ such that Liouvillian superoperator in projected subspaces matches the integrable models, the full spectrum of $\hat{\mathscr{L}}$ can be obtained analytically by solving each subspace individually.

Based on the above consideration, we consider a translationally invariant one-dimensional spin chain with length L, and the dissipation acts on the system locally. Then the Liouvillian superoperator is rewritten as

$$\begin{aligned}\hat{\mathscr{L}} =& -i\big(\hat{H}_S \otimes \hat{I} - \hat{I} \otimes \hat{H}_S^{\mathrm{T}}\big) + \sum_{j=1}^{L}\sum_{n=1}^{M}\big[2\hat{L}_j^{(n)} \otimes \hat{L}_j^{*(n)} \\ &- \hat{L}_j^{\dagger(n)}\hat{L}_j^{(n)} \otimes \hat{I} - \hat{I} \otimes \big(\hat{L}_j^{\dagger(n)}\hat{L}_j^{(n)}\big)^{\mathrm{T}}\big],\end{aligned} \tag{3}$$

where j is the site index and M denotes the number of dissipation channels on each site. In order to derive an exactly solvable Liouvillian superoperator, the choice of operators $\hat{L}_j^{(n)}$ and Hamiltonian $\hat{H}_S$ should guarantee the integrability of $\hat{\mathscr{L}}$. We first focus on the purely dissipative case, i.e., $\hat{H}_S = 0$. We choose the local dissipation channels to be $\hat{L}_j^{(1)} = \sqrt{J_L}\hat{S}_j^+\hat{S}_{j+1}^-$ and $\hat{L}_j^{(2)} = \sqrt{J_R}\hat{S}_{j+1}^+\hat{S}_j^-$, where $S_j^\pm$ is the local spin operator. Defining local projectors $\hat{\mathcal{P}}_j^1 = |1\rangle_j^R|0\rangle_j^L\langle 0|_j^L\langle 1|_j^R$, $\hat{\mathcal{P}}_j^2 = |0\rangle_j^R|1\rangle_j^L\langle 1|_j^L\langle 0|_j^R$, and $\hat{\mathcal{P}}_j^0 = 1 - \hat{\mathcal{P}}_j^1 - \hat{\mathcal{P}}_j^2$, where $|1\rangle$ and $|0\rangle$ denote spin up and down, respectively, and R and L operators act on the right and left Hilbert spaces, one can find easily $\hat{\mathcal{P}}_j^k\hat{\mathcal{P}}_j^l = \delta_{k,l}\hat{\mathcal{P}}_j^k$, and the Liouvillian superoperator commutes with these projectors.

Next, we consider the effective Liouvillian superoperator in projected subspaces. The most representative subspace is the diagonal subspace $\frac{d}{dt}\hat{\mathcal{P}}^0|\rho\rangle = \hat{\mathcal{P}}^0\hat{\mathscr{L}}|\rho\rangle = \hat{\mathscr{L}}_{\mathrm{eff}}\hat{\mathcal{P}}^0|\rho\rangle$, where $\hat{\mathcal{P}}^0 = \prod_j \hat{\mathcal{P}}_j^0$ and $\hat{\mathscr{L}}_{\mathrm{eff}} = \hat{\mathcal{P}}^0\hat{\mathscr{L}}\hat{\mathcal{P}}^0$. We now derive the effective Liouvillian $\hat{\mathscr{L}}_{\mathrm{eff}}$. First, we derive the effective action of individual $\hat{\mathscr{L}}$ terms:

$$\begin{aligned}\hat{\mathscr{L}}_{j,\mathrm{eff}}^{(1,2)} =& \hat{\mathcal{P}}^0\big[2\hat{L}_j^{(1,2)} \otimes \hat{L}_j^{*(1,2)} - \hat{L}_j^{\dagger(1,2)}\hat{L}_j^{(1,2)} \otimes \hat{I} \\ &- \hat{I} \otimes \big(\hat{L}_j^{\dagger(1,2)}\hat{L}_j^{(1,2)}\big)^T\big]\hat{\mathcal{P}}^0 \\ =& J_{L,R}\big[\hat{S}_j^+\hat{S}_{j+1}^- + \big(\hat{S}_j^z\hat{S}_{j+1}^z - \tfrac{1}{4}\big) \\ &+ \tfrac{1}{2}\big(\mp\hat{S}_j^z \pm \hat{S}_{j+1}^z\big)\big].\end{aligned} \tag{4}$$

From the Liouvillian (4), one can see clearly that nonreciprocal hopping derives from unequal dissipation strengths of $\hat{L}_j^{(1)}$ and $\hat{L}_j^{(2)}$. When adding $\hat{\mathscr{L}}_{j,\mathrm{eff}}^{(1)}$ and $\hat{L}_{j,\mathrm{eff}}^{(2)}$ terms together, the PBC ensures that the contribution of the last term vanishes. Further taking into account both $\hat{\mathscr{L}}_{j,\mathrm{eff}}^{(1,2)}$ terms, we arrive at the effective Liouvillian

$$\begin{aligned}\hat{\mathscr{L}}_{\mathrm{eff}} =& 2J\sum_{j=1}^{L}\Big[\frac{e^{-\phi}}{2}\hat{S}_j^+\hat{S}_{j+1}^- + \frac{e^{\phi}}{2}\hat{S}_{j+1}^+\hat{S}_j^- \\ &+ \cosh\phi\Big(\hat{S}_j^z\hat{S}_{j+1}^z - \frac{1}{4}\Big)\Big].\end{aligned} \tag{5}$$

Here we reset parameters J_L and J_R via J and ϕ ($J_L = Je^{-\phi}$, $J_R = Je^{\phi}$). The original parameter J_R (J_L) denotes the strength of up-spin hops to the right (left), and the PBC is adopted as schematically displayed in Fig. 1. We note that this model can be mapped to the Hatano-Nelson model [154] with

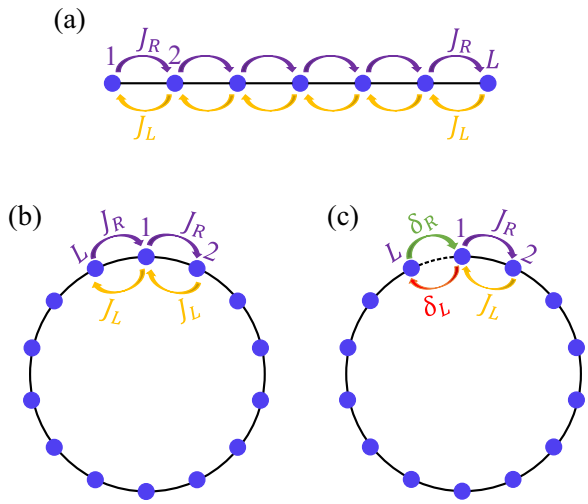

FIG. 1. Illustration of three boundary conditions. (a) The open boundary condition (OBC) with no hopping between two edges. (b) The periodic boundary condition (PBC). (c) The generalized boundary condition (GBC), where the hopping amplitudes are unequal to ones in the bulk ($\delta_L \neq J_L$, $\delta_R \neq J_R$.).

nearest-neighbor interaction by a Jordan-Wigner transformation. Without loss of generality, we assume $\phi > 0$, which means the right hopping is greater than the left. The solution of $\phi < 0$ is connected to the $\phi > 0$ case by inversion transformation $(\hat{S}_j^+, \hat{S}_j^-, \hat{S}_j^z) \to (\hat{S}_{L+1-j}^+, \hat{S}_{L+1-j}^-, \hat{S}_{L+1-j}^z)$. This model will be our main focus in the following discussion. A similar asymmetric non-Hermitian XXZ model is found to be exactly solvable under the PBC [155,156].

We move on now to consider other boundary conditions. For the OBC, as shown in Fig. 1(a), we can derive the following with the same procedure as in the PBC case. Following Eq. (4), we now have single $\hat{S}^z$ terms dangling at each end of the boundary:

$$\mathscr{L}_{\text{eff}}^{\text{OBC}} = J\sum_{j=1}^{L-1}\left[e^{\phi}\hat{S}_{j+1}^{+}\hat{S}_{j}^{-} + e^{-\phi}\hat{S}_{j}^{+}\hat{S}_{j+1}^{-} + 2\cosh\phi\left(\hat{S}_{j}^{z}\hat{S}_{j+1}^{z} - \frac{1}{4}\right)\right] + J\sinh\phi\left(\hat{S}_{L}^{z} - \hat{S}_{1}^{z}\right). \tag{6}$$

The effective model (6) is also exactly solvable since boundary terms preserve the $U(1)$ symmetry. Moreover, we further consider generalized boundary conditions (GBCs). The effective Liouvillian is derived by adding extra boundary terms from Eq. (4) to the OBC effective Liouvillian (6):

$$\begin{aligned}\mathscr{L}_{\text{eff}}^{\text{GBC}} =& J\sum_{j=1}^{L-1}\left[e^{\phi}\hat{S}_{j+1}^{+}\hat{S}_{j}^{-} + e^{-\phi}\hat{S}_{j}^{+}\hat{S}_{j+1}^{-} + 2\cosh\phi\left(\hat{S}_{j}^{z}\hat{S}_{j+1}^{z} - \frac{1}{4}\right)\right] + J\sinh\phi\left(\hat{S}_{L}^{z} - \hat{S}_{1}^{z}\right)\\ &+ \delta_L\left[\hat{S}_{L}^{+}\hat{S}_{1}^{-} + \left(\hat{S}_{L}^{z} - \frac{1}{2}\right)\left(\hat{S}_{1}^{z} + \frac{1}{2}\right)\right]\\ &+ \delta_R\left[\hat{S}_{1}^{+}\hat{S}_{L}^{-} + \left(\hat{S}_{1}^{z} - \frac{1}{2}\right)\left(\hat{S}_{L}^{z} + \frac{1}{2}\right)\right],\end{aligned} \tag{7}$$

with δ_L and δ_R being boundary couplings. The Liouvillian superoperator (7) is negative semidefinite, and its zero-energy eigenstate corresponds to the steady state. The OBC case is $\delta_L = \delta_R = 0$, and when $\delta_L = Je^{-\phi}$ and $\delta_R = Je^{\phi}$, the GBC goes back to the PBC case. Exploring the physical properties of the system under the GBC takes on special significance.

Before proceeding, we now discuss the effect of the system Hamiltonian part and other projected subspaces. The system Hamiltonian $\hat{H}_S$, as demonstrate above, should be chosen to ensure integrability in projected subspaces. Under the guidance of this principle, the integrability will be protected as long as the added Hamiltonian preserves the projected subspaces invariant and does not destroy the dissipation part. It is straightforward to write down a generic Hamiltonian of nearest-neighbor form, $\hat{H}_S = \sum_{j=1}^{L} J'\hat{S}_j^z\hat{S}_{j+1}^z + h\hat{S}_j^z$. The coherent term $\hat{H}_S \otimes \hat{I} - \hat{I} \otimes \hat{H}_S^{\mathrm{T}}$ is diagonal in different invariant subspaces since $\hat{S}_z$ does not flip a spin on each site, and the whole Liouvillian superoperator maintains its integrability. Under such circumstances, we then ignore the coherent term because it adds only a diagonal constant and has no influence on the subsequent discussion of the LSE. For other projected subspaces ($\hat{\mathcal{P}} \neq \hat{\mathcal{P}}^0$), the effective Liouvillian superoperators are connected to non-Hermitian XXZ chains with different parameters [140]. So in the rest of this paper, we study only the non-Hermitian XXZ model defined in Eqs. (5) through (7).

III. SOLUTION UNDER THE PERIODIC AND OPEN BOUNDARY CONDITIONS

This section will examine exact solutions of the Liouvillian superoperator under the PBC and OBC. Detailed analytical derivations are shown in Appendixes A and B. In the following we outline the main results.

We first deal with the PBC case. Since the number of up-spin particles $N_\uparrow$ or down-spin particles $N_\downarrow$ is a conserved quantity, we can solve the non-Hermitian XXZ model individually in different subspaces with fixed $(N_\uparrow, N_\downarrow)$:

$$|\psi\rangle = \sum_{j=1}^{M}\sum_{x_j=1}^{L}\varphi(x_1, x_2, \ldots, x_M)S_{x_1}^{+}S_{x_2}^{+}\cdots S_{x_M}^{+}|\text{vac}\rangle, \tag{8}$$

where $|\text{vac}\rangle = |\downarrow\downarrow\cdots\downarrow\rangle$ denotes the vacuum (no boson excited) state and $M = N_\uparrow$. The wave function $\varphi(x_1, x_2, \ldots, x_M)$ is expressed by the Bethe ansatz form

$$\varphi(x_1, x_2, \ldots, x_M) = \sum_{\mathbf{P}} A_{\mathbf{P}} \exp\left(i\sum_{j=1}^{M} k_{p_j}x_j\right), \tag{9}$$

where $\{k_j\}$ is the quasimomentum and the eigenspectrum (dispersion relation) is determined with respect to the quasimomentum,

$$E = E_0 + 2J\sum_{j=1}^{M}[\cos(k_j + i\phi) - \cosh\phi], \tag{10}$$

where the quasimomenta are determined by the Bethe ansatz equations (BAEs) (A7). By solving the BAEs, we get the gapless excitation spectrum, which resembles the behavior of the Hermitian XXZ model in the gapless phase.

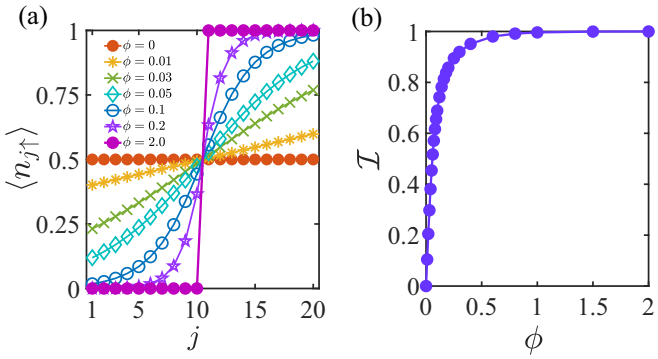

FIG. 2. LSE in the OBC at half filling. (a) The occupation number of the spin up at each site for different ϕ. (b) Spin imbalance $\mathcal{I}$ as a function of ϕ. Here we choose the system length $L = 20$, and the number of up spins $M = 10$.

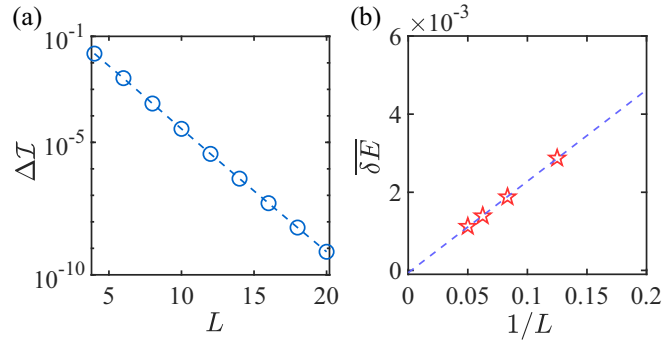

FIG. 3. Comparison of the GBC and OBC for imbalance and spectrum. (a) The imbalance deviation $\Delta\mathcal{I}$ between the GBC ($\delta_L \neq 0$, $\delta_R = 0$) and the OBC cases as a function of system size L. Here we choose $M = L/2$, $\phi = 0.5$, and $\delta_L = 0.5J_L$. (b) Finite size scaling of the mean energy level difference $\overline{\delta E}$ between the GBC ($\delta_L \neq 0$, $\delta_R = 0$) and OBC for $M = L/4$.

Actually, Ref. [155] pointed out that if one considers an artificial non-Hermitian XXZ model with tunable S^z coupling, the model undergoes a phase transition from gapless to gapped phases if one increases ϕ while maintaining the S^z coupling. However, the physical effective Liouvillian considered in our paper has the property that magnon hopping strength is related to S^z coupling, so the system remains in the gapless phase for any nonzero ϕ. This means that the non-Hermitian XXZ model considered here is in the same phase as the Hermitian gapless phase. Their ground states thus have no qualitative difference. The difference between Hermitian and non-Hermitian models is only that the latter has a complex spectrum.

For the OBC case, the non-Hermitian XXZ model (6) can also be exactly solved as long as a matched ansatz is chosen. Starting from the ansatz

$$\varphi(x_1, x_2, \ldots, x_M) = \sum_{\mathbf{P}, \mathbf{r_1}, \ldots, \mathbf{r_M}} A_{\mathbf{P}}(r_1, r_2, \ldots, r_M) \times \exp\left[\sum_{j=1}^{M} \left(i r_j k_{p_j} x_j + \phi x_j\right)\right], \quad (11)$$

where $r_j = \pm 1$ denotes waves reflected by the boundary, one can obtain the exact dispersion relation $E = J\sum_{j=1}^{M}[\cos(k_j) - \cosh\phi]$ and BAEs (B5). Remarkably, both the dispersion relation and BAEs under the OBC are the same as those of the Hermitian counterpart in (B7). This feature, in fact, can be understood through an imaginary gauge transformation, $\hat{S}_j^+ \to e^{-j\phi}\hat{S}_j^+$, $\hat{S}_j^- \to e^{j\phi}\hat{S}_j^-$, and $\hat{S}_j^z \to \hat{S}_j^z$, which transforms the non-Hermitian XXZ model (6) to its Hermitian counterpart (B7); meanwhile, the wave function gets an exponential factor $e^{\sum_{j=1}^{M}\phi x_j}$. Remarkably, in this case the excitation spectrum is gapped, distinct from the PBC case.

Owing to this exponential weight, the spin-up (boson) tends to be more concentrated than in the Hermitian case, resulting in the appearance of the LSE. Figure 2(a) shows the density distribution of the steady state for different ϕ for the half-filling case, from which we can see the skin effect appears. To quantitatively describe the LSE, we introduce the spin imbalance $\mathcal{I} = \frac{N_{\uparrow,r} - N_{\uparrow,l}}{N_{\uparrow,r} + N_{\uparrow,l}}$, where $N_{\uparrow,l}, N_{\uparrow,r}$ ($N_{\uparrow,r}, N_{\downarrow,r}$) is the number of up spins in the left (right) half of the lattice. In the limit $\phi \to 0$, spins are uniformly distributed on the lattice. With the growth of ϕ, up-spin particles tend toward occupying part of the lattice near the right boundary, and the spin imbalance $\mathcal{I}$ rises from 0 to 1 [see Fig. 2(b)]. This means that, under the OBC, the system ultimately relaxes to the steady state with the LSE, regardless of the choice of initial states. Physically, the asymmetric hopping causes a spin current, leading to the up spins congregating near the right boundary.

IV. SOLUTION UNDER GENERALIZED BOUNDARY CONDITIONS

In this section, we focus on the GBC and investigate the fate of the LSE as additional boundary terms are inserted. For the sake of convenience, we first study the situation in which a counterflow boundary hopping ($\delta_L \neq 0$, $\delta_R = 0$) is added to the Liouvillian:

$$\hat{\mathscr{L}}_{\text{left}} = J\sum_{j=1}^{L-1}\left[e^{\phi}\hat{S}_{j+1}^+\hat{S}_j^- + e^{-\phi}\hat{S}_j^+\hat{S}_{j+1}^- + 2\cosh\phi\left(\hat{S}_j^z\hat{S}_{j+1}^z - \frac{1}{4}\right)\right] + J\sinh\phi\left(\hat{S}_L^z - \hat{S}_1^z\right) + \delta_L\left[\hat{S}_L^+\hat{S}_1^- + \left(\hat{S}_L^z - \frac{1}{2}\right)\left(\hat{S}_1^z + \frac{1}{2}\right)\right]. \quad (12)$$

We will see that results in this situation are the same as those in the OBC case in the thermodynamic limit. In order to verify this, we calculate the imbalance difference $\Delta\mathcal{I} = \mathcal{I}_{\text{left}} - \mathcal{I}_{\text{OBC}}$ for the steady state between the Liouvillian (12) and (6). As illustrated in Fig. 3(a), the imbalance difference exponentially vanishes with increasing of the system size L. This means the LSE survives in the presence of counterflow boundary hopping. The reason the boundary term δ_L does not spoil the LSE can be understood through a simple physical picture. in the large-ϕ limit, the steady state approaches to the state $|\downarrow\rangle_1|\downarrow\rangle_2\cdots|\downarrow\rangle_{L-M}|\uparrow\rangle_{L-M+1}|\uparrow\rangle_{L-M+2}\cdots|\uparrow\rangle_L$, the boundary hopping is forbidden, and meanwhile, the right hopping in the bulk has no effect on the domain wall.

For finite ϕ, we apply the gauge transformation $\hat{S}_j^+ \to e^{-j\phi}\hat{S}_j^+$, $\hat{S}_j^- \to e^{j\phi}\hat{S}_j^-$, and $\hat{S}_j^z \to \hat{S}_j^z$, as done in the OBC case. Then the Liouvillian (12) turns into the Hermitian counterpart of the OBC (B7) plus a boundary term, $\delta_L e^{-\phi L}\hat{S}_L^+\hat{S}_1^- + \delta_L(\hat{S}_L^z - \frac{1}{2})(\hat{S}_1^z + \frac{1}{2})$, where the effect caused by boundary hopping term $\hat{S}_L^+\hat{S}_1^-$ is exponentially small. This conclusion is supported by the result in Fig. 3(a). Another term, $\delta_L(\hat{S}_L^z - \frac{1}{2})(\hat{S}_1^z + \frac{1}{2})$, is Hermitian and just serves as a boundary potential which does not flip boundary spins. This will bring out a $1/L$ correction in the spectrum. To discern this, we calculate the mean energy level difference $\overline{\delta E} = \overline{E}_{\text{left}} - \overline{E}_{\text{OBC}}$ between the Liouvillian (12) and (6). Here the mean energy is defined by $\overline{E} = \sum_j \overline{E}_j$, with $\overline{E}_j = \frac{E_j - E_{\min}}{E_{\max} - E_{\min}}$, where $E_{\max}$ ($E_{\min}$) denotes the maximum (minimum) eigenvalue. The finite size scaling of $\overline{\delta E}$ as plotted in Fig. 3(b) displays the $1/L$ correction as expected.

We move on now to consider the more general situation, i.e., neither δ_L nor δ_R is zero. First, we find that coflow boundary hopping strength δ_R is exponentially amplified ($\delta_R e^{\phi L}\hat{S}_1^+\hat{S}_L^-$) if one employs the gauge transformation done above. This implies that we cannot extract the correct consequences from the gauge transformation, indicating that the wave function ansatz under the OBC has failed because it no longer matches boundary conditions induced by δ_R. In fact, as shown in Appendix C, in the thermodynamic limit, the eigenfunction necessarily takes the form of a PBC-like wave function instead of the OBC-like one. Concretely, the PBC-like eigenfunction dismisses the LSE and consists of modified plane waves $\lambda^{\frac{x_j}{L}} e^{ik_{P_j}x_j}$ instead of the original plane waves. The amplitudes of the modified plane waves depend on the ratio $\lambda = Je^{\phi}/\delta_R$, leading to the density distribution at the right boundary ($x_j = L$) being only λ times greater than that at the left boundary ($x_j = 1$), which fundamentally differs from the OBC case, where the LSE manifests in the exponential amplifier $e^{\phi L}$ of the density distribution. In order to characterize the distinction between them, we compute the ratio of up-spin particle numbers between the right and left boundaries $\langle n_{L\uparrow}\rangle/\langle n_{1\uparrow}\rangle$, as illustrated in Figs. 4(a) and 4(b). For the case of the GBC with $\delta_R = 0$, the ratio is exponentially divergent due to the LSE, while it remains a finite value for the GBC with $\delta_R \neq 0$, showing the absence of the LSE. Moreover, the distinction is also reflected in the imbalance of eigenstates. If we introduce mean imbalance $\overline{\mathcal{I}} = \sum_n \mathcal{I}_n/\mathcal{D}$, where $\mathcal{I}_n$ denotes the imbalance of the nth eigenstate, a significant difference can be visualized from Figs. 4(c) and 4(d).

For the GBC ($\delta_R = 0$), $\overline{\mathcal{I}}$ gradually approaches 1 as the system size grows since eigenstates exhibit the LSE, but it is nearly constant once a finite $\delta_R \neq 0$ is involved. That is to say, the LSE is fragile under the perturbation of coflow boundary hopping δ_R but can survive the counterflow term δ_L. To see this more clearly, we investigate the parameter variations from the vanishing coflow boundary coupling $\delta_R/J_R = 0$ to the full coflow boundary coupling $\delta_R/J_R = 1$ with a fixed counterflow strength $\delta_L/J_L = 1$. This corresponds to the transition from the GBC with $\delta_R = 0$ and $\delta_L \neq 0$ to the PBC. Figure 5(a) plots the occupation number of up-spin particles at half filling, which shows that almost all up spins occupy the right half of

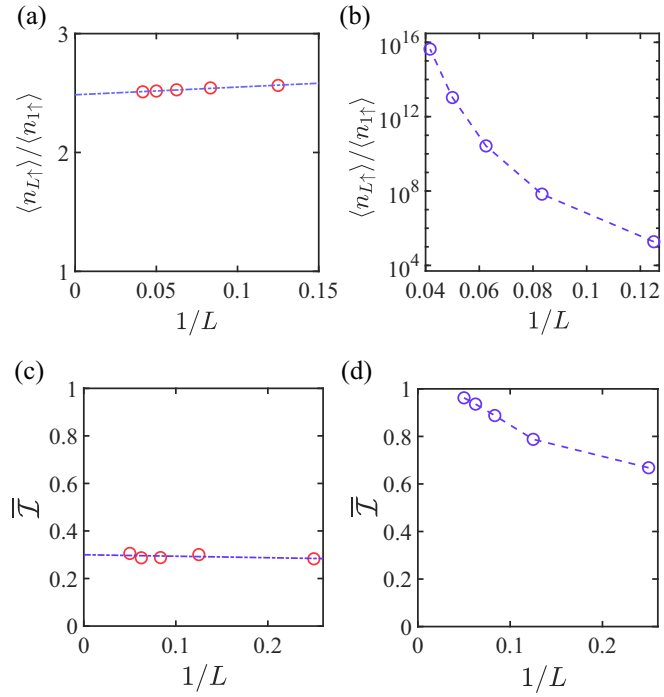

FIG. 4. Comparison of (a) and (b) the occupation ratio $\langle n_{L\uparrow}\rangle/\langle n_{1\uparrow}\rangle$ in the steady state and (c) and (d) mean imbalance $\overline{\mathcal{I}}$ as a function of $1/L$ for two different GBCs. (a) and (c) plot the results of the GBC ($\delta_L \neq 0$, $\delta_R \neq 0$), and the OBC case ($\delta_L \neq 0$, $\delta_R = 0$) is plotted in (b) and (d). Here we choose $M = L/2$, $\phi = 0.5$, $\delta_L = 0.5J_L$, and $\delta_R = 0.5J_R$ for (a) and (c) and $M = L/2$, $\phi = 0.5$, $\delta_L = 0.5J_L$, and $\delta_R = 0$ for (b) and (d).

the lattice exhibiting the LSE when $\delta_R = 0$. As coflow boundary coupling δ_R increases, the occupation number smooths gradually and eventually reaches a discrete uniform distribution in the PBC case $\delta_L/J_L = 1$. To examine the fate of the LSE further, we calculate the occupation ratio between the

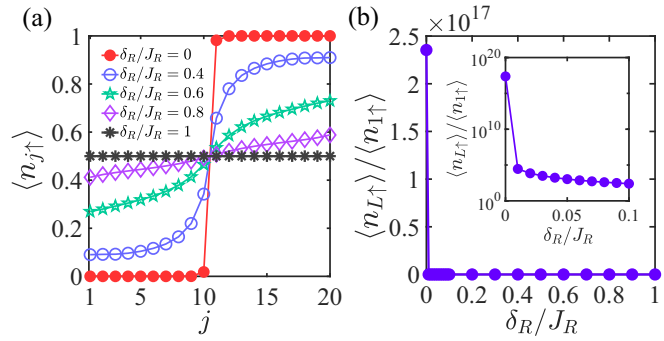

FIG. 5. LSE in boundary conditions transitioning from the GBC to PBC at half filling. (a) The occupation number of up-spin particles at each site for different δ_R. (b) The occupation ratio $\langle n_{L\uparrow}\rangle/\langle n_{1\uparrow}\rangle$ for different δ_R. The inset shows a single-logarithm plot where the ratio for $\delta_R = 0$ has an exponential magnitude but follows a power law for finite $\delta_R \neq 0$. Here we choose system length $L = 20$, $M = L/2$, and $\delta_L/J_L = 1$. The parameter choice $\delta_L/J_L = 1$ means that the system is in the PBC when $\delta_R/J_R = 1$.

right and left boundaries $\langle n_{L\uparrow}\rangle/\langle n_{1\uparrow}\rangle$, as shown in Fig. 5(b). One can see clearly that an exponentially divergent ratio $e^{\phi L}$ appear in $\delta_R = 0$, which means the LSE exists, while the LSE vanishes for any finite coflow boundary term $\delta_R \neq 0$ since $\langle n_{L\uparrow}\rangle/\langle n_{1\uparrow}\rangle$ is just algebraically related to J_R/δ_R and tends toward being finite in the thermodynamic limit [see Fig. 4(a)].

V. SUMMARY AND OUTLOOK

In summary, using the non-Hermitian XXZ model as an example of exactly solvable many-body Liouvillian superoperators, we detailedly solved the model under various boundary conditions utilizing the Bethe ansatz, which enabled us to investigate the existence condition of the LSE under different boundary conditions. The main conclusions are summarized as follows. First, for the PBC in which no LSE occurs, there is no phase transition (gap closing) in the system. Second, for the OBC, the wave function is intrinsically distinct from the PBC one due to the existence of the LSE. We identified the LSE by investigating the density distribution and spin imbalance. We then explored the fate of the LSE in the presence of boundary hoppings. The LSE survives in a kind of GBC with nonzero counterflow hopping at the boundary because the exact solutions, in this case, are equivalent to those of the OBC in the thermodynamic limit. In contrast, the LSE will be destroyed immediately once a coflow hopping appears at the boundary, with goes back to the similarity to solutions in the PBC. An obvious fact is that boundary conditions will have no consequences on the system in thermodynamic limit. This is, indeed, true in Hermitian systems. For open quantum systems, which are intrinsically non-Hermitian, the properties of the system could strongly depend on the boundary condition, even in the thermodynamic limit. This paper is a beneficial endeavor to understand the LSE in exactly solvable open quantum many-body systems. These results add to the expanding field of open quantum systems and could provide a deeper understanding of the non-Hermitian realm. Further studies are desired to explore the integrability of many-body Liouvillian superoperators, especially under constraint boundary conditions. Generally, the existing literature mainly deals with those non-Hermitian models whose Hermitian parts are integrable. However, a recent study [149] found that a particular non-Hermitian Bose-Hubbard model with unidirectional hopping turned out to be integrable, although the Bose-Hubbard model itself is not integrable and cannot be analytically solved. This discovery opens the avenue for further explorations and would produce exciting findings in open many-body quantum systems.

ACKNOWLEDGMENTS

The work is supported by the National Natural Science Foundation of China (Grants No. 12304290 and No. 12304388) and the National Key Research and Development Program of China (Grants No. 2023YFA1406704 and No. 2022YFA1405800). L.P. also acknowledges support from the Fundamental Research Funds for the Central Universities.

APPENDIX A: EXACT SOLUTION FOR THE NON-HERMITIAN XXZ MODEL IN PERIODIC BOUNDARY CONDITION

In this Appendix, we solve the non-Hermitian XXZ model under the periodic boundary condition (PBC) by means of the Bethe ansatz. The model is written as

$$\hat{\mathscr{L}} = 2J\sum_{j=1}^{L}\left[\frac{e^{-\phi}}{2}\hat{S}_j^+\hat{S}_{j+1}^- + \frac{e^{\phi}}{2}\hat{S}_{j+1}^+\hat{S}_j^- + \cosh\phi\left(\hat{S}_j^z\hat{S}_{j+1}^z - \frac{1}{4}\right)\right], \tag{A1}$$

where $\phi > 0$ denotes the nonreciprocal spin hopping and the PBC is applied ($\hat{S}_{L+1}^{x,y,z} = \hat{S}_1^{x,y,z}$). Now we show that this non-Hermitian XXZ model (A1) can be exactly solved by the Bethe ansatz. According to the standard procedure of the Bethe ansatz, we start from the reference state

$$|\,\mathrm{Vac}\rangle = |\downarrow\downarrow\cdots\downarrow\rangle, \tag{A2}$$

which satisfies $\hat{\mathscr{L}}|\,\mathrm{Vac}\rangle = E_0|\,\mathrm{vac}\rangle$, with $E_0 = 0$. This means the reference state is the steady state of the Lindbladian. Writing the eigenfunction in the $S^Z = M - \frac{L}{2}$ sector with the number of down-spin particles M (without loss of generality, we set $M \leqslant \frac{L}{2}$),

$$|\psi\rangle = \sum_{j=1}^{M}\sum_{x_j=1}^{L}\varphi(x_1, x_2, \ldots, x_M)S_{x_1}^+S_{x_2}^+\cdots S_{x_M}^+|\mathrm{vac}\rangle. \tag{A3}$$

We restrict the state to the region $1 < x_1 < x_2 < \cdots < x_M < L$ since states in other regions can be obtained by permutation symmetry.

According to the eigenequation $\hat{\mathscr{L}}|\psi\rangle = E|\psi\rangle$, one can derive the following relation:

$$J\sum_j\left(1-\delta_{x_j+1,x_{j+1}}\right)[\psi(x_1,\ldots,x_j+1,x_{j+1},\ldots,x_M)e^{-\phi} + \psi(x_1,\ldots,x_j,x_{j+1}-1,\ldots,x_M)e^{\phi}] + \left[E_0 - E - 2J\cosh\phi\left(M - \sum_j\delta_{x_j+1,x_{j+1}}\right)\right]\varphi(x_1,x_2,\ldots,x_M) = 0. \tag{A4}$$

Constructing the many-body wave function by means of the Bethe ansatz form

$$\varphi(x_1, x_2, \ldots, x_M) = \sum_{\mathbf{P}} A_{\mathbf{P}}\exp\left(i\sum_{j=1}^{M}k_{p_j}x_j\right), \tag{A5}$$

where $\mathbf{P} = (p_1, p_2, \ldots, p_M)$ is a permutation of $1, 2, \ldots, M$, yields the eigenvalue

$$E = E_0 + 2J\sum_{j=1}^{M}[\cos(k_j + i\phi) - \cosh\phi] \tag{A6}$$

and the Bethe ansatz equations

$$\exp(ik_jL) = (-1)^{M-1}\prod_{l\neq j}^{M}\frac{\exp[i(k_j+k_l)-2\phi]+1-2\cosh\phi\exp(ik_j-\phi)}{\exp[i(k_j+k_l)-2\phi]+1-2\cosh\phi\exp(ik_l-\phi)} \tag{A7}$$

via the PBC $\varphi(x_1, x_2, \ldots, x_M) = \varphi(x_2, \ldots, x_M, x_1 + L)$. For the sake of convenience, introducing rapidity parameters $\{\lambda_j\}$,

$$\exp(ik_j - \phi) = -\frac{\sin[\phi(\lambda_j + i)/2]}{\sin[\phi(\lambda_j - i)/2]}, \tag{A8}$$

(A7) becomes

$$\left[\frac{\sin\frac{\phi}{2}(\lambda_j+i)}{\sin\frac{\phi}{2}(\lambda_j-i)}\right]^L e^{\phi L} = \prod_{l\neq j}^{M}\frac{\sin\frac{\phi}{2}(\lambda_j-\lambda_l+2i)}{\sin\frac{\phi}{2}(\lambda_j-\lambda_l-2i)}. \tag{A9}$$

Taking the logarithm of the above equations, we obtain

$$L\theta_1(\lambda_j) = 2\pi I_j + i\phi L + \sum_{l\neq j}^{M}\theta_2(\lambda_j - \lambda_l), \tag{A10}$$

where $\theta_n(\lambda) = 2\arctan[\tan(\frac{\phi\lambda}{2})\coth(\frac{n\phi}{2})]$. For the ground state $(M = \frac{L}{2})$, we have $I_j = -(\frac{L}{2}-1)/2, -(\frac{L}{2}-1)/2+1, \ldots, (\frac{L}{2}-1)/2-1, (\frac{L}{2}-1)/2$. In the thermodynamic limit $L \to \infty$, Eq. (A10) becomes

$$2\theta_1(\lambda) = 2\pi\int^{\lambda}\sigma(\lambda')d\lambda' + i\phi + 2\int_{\mathcal{C}}\theta_2(\lambda-\lambda')\sigma(\lambda')d\lambda', \tag{A11}$$

where $\mathcal{C}$ is the rapidity path in the complex plain. Since θ_1 is a function with a period of $\frac{2\pi}{\phi}$, one can restrict the domain of definition to $\frac{\pi}{\phi} \leqslant \mathrm{Re}\,\lambda \leqslant \frac{\pi}{\phi}$. Differentiating (A11), the distribution $\sigma(\lambda)$ satisfies the equation

$$\frac{\phi\sinh\phi}{\cosh\phi - \cos(\phi\lambda)} = 2\pi\sigma(\lambda) + \int_{\mathcal{C}}\frac{\phi\sinh(2\phi)}{\cosh(2\phi)-\cos[\phi(\lambda-\lambda')]}\sigma(\lambda')d\lambda', \tag{A12}$$

from which one can find two poles $\Rightarrow \lambda - \lambda' = \pm 2i$ in the integrand. If $-1 < \mathrm{Im}\,\lambda < 1$ and $-1 < \mathrm{Im}\,\lambda' < 1$, then the integral path dose not enclose poles, which means the path can be continuously deformed to the real axis. As ϕ grows, the path $\mathcal{C}$ gradually extends to the complex plane and then touches poles when $\phi = \phi_c$, in which case Eq. (A11) diverges and the mass gap is closed [155].

Next, we calculate the critical value ϕ_c. When $\phi < \phi_c$, the poles are not enclosed by curve $\mathcal{C}$, and the integral path can be continuously deformed to the real axis, in which case

$$\frac{\phi\sinh\phi}{\cosh\phi - \cos(\phi\lambda)} = 2\pi\sigma(\lambda) + \int_{-\frac{\pi}{\phi}}^{\frac{\pi}{\phi}}\frac{\phi\sinh(2\phi)}{\cosh(2\phi)-\cos[\phi(\lambda-1)]}\sigma(\Lambda)d\lambda. \tag{A13}$$

We can solve $\sigma(\lambda)$ by performing the Fourier transformation of Eq. (A13).

$$\sigma(\lambda) = \sum_{m=-\infty}^{\infty}\frac{e^{-im\phi\lambda}}{2\cosh(m\phi)}. \tag{A14}$$

After substituting Eq. (A14) into Eq. (A11) and considering the expansion

$$\theta_1(\lambda) = \phi\lambda - \sum_{m\neq 0}\frac{\exp(-im\phi\lambda - \phi|n|)}{im\phi},$$
$$\theta_2(\lambda) = \phi\lambda - \sum_{m\neq 0}\frac{\exp(-im\phi\lambda - 2\phi|n|)}{im\phi}, \tag{A15}$$

we obtain the equation

$$\phi = 2\pi iZ(\lambda) + \frac{\phi}{2}b - \frac{i}{2}\phi\lambda + \sum_{m\neq 0}\frac{e^{-im\phi}}{2m\cosh(m\phi)} + \sum_{m\neq 0}(-1)^m\frac{e^{m\phi b}}{2m\cosh(m\phi)}. \tag{A16}$$

The critical value ϕ_c is determined by $\lambda = \pm\frac{\pi}{\phi} + i$,

$$\phi = \phi + \sum_{m=1}^{\infty}\frac{(-1)^m\tanh(m\phi)}{m}, \tag{A17}$$

from which we find there is only a trivial solution $\phi_c = 0$. That means no gap closing happens.

APPENDIX B: EXACT SOLUTION FOR THE NON-HERMITIAN XXZ MODEL UNDER OPEN BOUNDARY CONDITIONS

In this Appendix, we discuss the non-Hermitian XXZ model under the OBC, which exhibits the skin effect. In the OBC, the Liouvillian is expressed as

$$\hat{\mathscr{L}}_{\mathrm{OBC}} = J\sum_{j=1}^{L-1}\left[e^{\phi}\hat{S}_{j+1}^{+}\hat{S}_{j}^{-} + e^{-\phi}\hat{S}_{j}^{+}\hat{S}_{j+1}^{-} + 2\cosh\phi\left(\hat{S}_{j}^{z}\hat{S}_{j+1}^{z} - \frac{1}{4}\right)\right] + J\sinh\phi\left(\hat{S}_{L}^{z} - \hat{S}_{1}^{z}\right). \tag{B1}$$

For simplicity, we first discuss the limit $\phi \to \infty$, in which the Liouvillian can be reduced to the following form (in units of e^{ϕ}):

$$\hat{\mathscr{L}}_{\mathrm{OBC}} = J\sum_{j=1}^{L-1}\left[S_{j+1}^{+}\hat{S}_{j}^{-} + \left(\hat{S}_{j}^{z}\hat{S}_{j+1}^{z} - \frac{1}{4}\right)\right] + \frac{J}{2}\left(\hat{S}_{L}^{z} - \hat{S}_{1}^{z}\right). \tag{B2}$$

Notably, the matrix representation of the Liouvillian (B2) is a triangular matrix in the basis

$$\{|\downarrow\cdots\downarrow\downarrow\uparrow\uparrow\cdots\uparrow\rangle, |\downarrow\cdots\downarrow\uparrow\downarrow\uparrow\cdots\uparrow\rangle, |\uparrow\uparrow\cdots\uparrow\downarrow\uparrow\downarrow\downarrow\cdots\downarrow\rangle\cdots, |\uparrow\uparrow\cdots\uparrow\downarrow\uparrow\downarrow\downarrow\cdots\downarrow\rangle, |\uparrow\uparrow\cdots\uparrow\downarrow\downarrow\cdots\downarrow\rangle\}, \tag{B3}$$

in which case it can easily be diagonalized. One can find that the state $|\downarrow\rangle_1|\downarrow\rangle_2\cdots|\downarrow\rangle_M|\uparrow\rangle_{M+1}|\uparrow\rangle_{M+2}\cdots|\uparrow\rangle_L$ where a spin domain-wall plateau emerges, is the exact eigenstate. This eigenstate is also a steady state because it has zero eigenvalue. This means that the system relaxes eventually to the skin mode, where all up spins (bosons) are arranged in right sites. For the finite ϕ, the Liouvillian (B1) is solvable with the Bethe ansatz. Here it should be emphasized that the Liouvillian (B1) cannot be solved simply in terms of the traditional Bethe ansatz for the Hermitian case in the OBC, i.e., $\varphi(x_1, x_2, \ldots, x_M) = \sum_{\mathbf{P},\mathbf{r}_1,\ldots,\mathbf{r}_M} A_{\mathbf{P}}(r_1, r_2, \ldots, r_M)\exp(\sum_{j=1}^{M} ik_{p_j}x_j)$. One should adopt the following ansatz:

$$\varphi(x_1, x_2, \ldots, x_M) = \sum_{\mathbf{P},\mathbf{r}_1,\ldots,\mathbf{r}_M} A_{\mathbf{P}}(r_1, r_2, \ldots, r_M) \times \exp\left[\sum_{j=1}^{M}(ir_j k_{p_j}x_j + \phi x_j)\right], \tag{B4}$$

where $r_j = \pm 1$ denotes the plane wave of the jth particle traveling toward the left ($r_j = -1$) and right ($r_j = 1$). In this way, after some calculations, one can obtain the following Bethe ansatz equations:

$$e^{i2(L-1)k_j}\frac{\left(e^{ik_j} - \sinh\phi - \cosh\phi\right)\left(e^{ik_j} + \sinh\phi - \cosh\phi\right)}{\left(e^{-ik_j} - \sinh\phi - \cosh\phi\right)\left(e^{-ik_j} + \sinh\phi - \cosh\phi\right)} = \prod_{l\neq j}^{M}\frac{S(-k_j, k_l)S(k_l, k_j)}{S(k_j, k_l)S(k_l, -k_j)}, \tag{B5}$$

with $S(k_j, k_l) = 1 - 2\cosh\phi e^{ik_l} + e^{i(k_j+k_l)}$ and the associated eigenvalues

$$E = 2J\sum_{j=1}^{M}[\cos(k_j) - \cosh\phi]. \tag{B6}$$

One can find that the BAEs and eigenvalues are identical to those in the Hermitian XXZ model under the OBC, and the only difference between them exists in the wave function, where ϕ will appear in the non-Hermitian system, as shown in Eq. (B4). In order to understand this, we employ the gauge transformation $\hat{S}_j^{+} \to e^{-j\phi}\hat{S}_j^{+}$, $\hat{S}_j^{-} \to e^{j\phi}\hat{S}_j^{-}$, and $\hat{S}_j^{z} \to \hat{S}_j^{z}$ to eliminate the unequal hopping which reproduces the Hermitian counterpart

$$\hat{\mathscr{L}}_{\mathrm{Hermitian}} = J\sum_{j=1}^{L-1}\left[\hat{S}_{j+1}^{+}\hat{S}_{j}^{-} + \hat{S}_{j}^{+}\hat{S}_{j+1}^{-} + 2\cosh\phi\left(\hat{S}_{j}^{z}\hat{S}_{j+1}^{z} - \frac{1}{4}\right)\right] + J\sinh\phi\left(\hat{S}_{L}^{z} - \hat{S}_{1}^{z}\right). \tag{B7}$$

Thus, it is straightforward that for the Hermitian XXZ model (B7), BAEs and eigenvalues are given by Eqs. (B5) and (B6). But the wave function to be changed correspondingly, $\varphi(x_1, x_2, \ldots, x_M) \to \varphi(x_1, x_2, \ldots, x_M)e^{\sum_{j=1}^{M}\phi x_j}$, is nothing but the ansatz (B4). This implies that the NHSE exists under the OBC because the solution of k_j is identical to the Hermitian case which is determined by BAEs (B7) and the wave function captures the exponential factor.

APPENDIX C: EXACT SOLUTION FOR THE NON-HERMITIAN XXZ MODEL UNDER GENERALIZED BOUNDARY CONDITIONS

After solving the non-Hermitian XXZ model under the PBC and OBC, we discuss other situations in which one unidirectional hopping term appears at the boundary. We first investigate the situation in which the Liouvillian is expressed as

$$\hat{\mathscr{L}}_{\mathrm{left}} = J\sum_{j=1}^{L-1}\left[e^{\phi}\hat{S}_{j+1}^{+}\hat{S}_{j}^{-} + e^{-\phi}\hat{S}_{j}^{+}\hat{S}_{j+1}^{-} + 2\cosh\phi\left(\hat{S}_{j}^{z}\hat{S}_{j+1}^{z} - \frac{1}{4}\right)\right] + J\sinh\phi\left(\hat{S}_{L}^{z} - \hat{S}_{1}^{z}\right) + \delta_L\left[\hat{S}_{L}^{+}\hat{S}_{1}^{-} + \left(\hat{S}_{L}^{z} - \frac{1}{2}\right)\left(\hat{S}_{1}^{z} + \frac{1}{2}\right)\right]. \tag{C1}$$

Here $\delta_L\hat{S}_L^{+}\hat{S}_1^{-}$ denotes the unidirectional hopping from the left to the right boundary.

Starting from the OBC ansatz (B4), since the boundary hopping term has no impact on the bulk spins, the eigenenergy is the same as in the OBC case (B6). However, it is expected that the boundary equations will be modified, and a straightforward

calculation gives

$$J\sum_{j=2}^{M}\sum_{\delta=\pm1}\left(1-\delta_{x_j+\delta,x_{j+\delta}}\right)\phi(1,\ldots,x_j+\delta,\ldots,x_M)e^{-\delta\phi}-\left[E+2J\cosh\phi\left(M-1/2-\sum_{j=2}^{M}\delta_{x_j+1,x_{j+1}}\right)\right]\varphi(1,x_2,\ldots,x_M)$$
$$+Je^{-\phi}\varphi(2,x_2,\ldots,x_j,\ldots,x_M)-(J\sinh\phi+\delta_L)\,\varphi(1,x_2,\ldots,x_j,\ldots,x_{M-1},x_M)=0, \tag{C2a}$$

$$J\sum_{j=1}^{M-1}\sum_{\delta=\pm1}\left(1-\delta_{x_j+\delta,x_{j+\delta}}\right)\phi(x_1,\ldots,x_j+\delta,\ldots,L)e^{-\delta\phi}-\left[E+2J\cosh\phi\left(M-1/2-\sum_{j=1}^{M-1}\delta_{x_j+1,x_{j+1}}\right)\right]\varphi(x_1,x_2,\ldots,L)$$
$$+Je^{\phi}\sum_{j=1}^{M-1}\varphi(x_1,\ldots,x_j,\ldots,L-1)+\underset{\sim}{\delta_L\varphi(1,x_1,\ldots,x_j,\ldots,x_{M-1})}+J\sinh\phi\,\varphi(x_1,\ldots,x_j,\ldots,x_{M-1},L)=0, \tag{C2b}$$

where the term marked with the wavy line originates from the boundary hopping term. From the OBC ansatz (B4), one can find the boundary hopping term is exponentially smaller than other terms since they are amplified with a factor $e^{L\phi}$. This means that the boundary term vanishes in the thermodynamic limit, which indicates solutions are identical to those of the OBC case. Hence, it is reasonably concluded that the system exhibits the NHSE where up-spin particles accumulate toward the right boundary. An alternative explanation for the NHSE existing in this system is that in the large-ϕ limit, similar to the OBC case, the state $|\downarrow\rangle_1|\downarrow\rangle_2\cdots|\downarrow\rangle_M|\uparrow\rangle_{M+1}|\uparrow\rangle_{M+2}\cdots|\uparrow\rangle_L$ is a zero-energy eigenstate because the boundary hopping term has no effect on it.

We now turn to discuss the generalized boundary condition with $\delta_L\neq0$ and $\delta_R\neq0$, as shown in Eq. (7). In this case, the boundary equations are given by

$$J\sum_{j=2}^{M}\sum_{\delta=\pm1}\left(1-\delta_{x_j+\delta,x_{j+\delta}}\right)\varphi(1,\ldots,x_j+\delta,\ldots,x_M)e^{-\delta\phi}-\left[E+2J\cosh\phi\left(M-1/2-\sum_{j=2}^{M}\delta_{x_j+1,x_{j+1}}\right)\right]\varphi(1,x_2,\ldots,x_M)$$
$$+Je^{-\phi}\varphi\big(2,x_2,\ldots,x_j,\ldots,x_M\big)+\underset{\sim}{\delta_R\varphi(x_2,\ldots,x_j,\ldots,x_M,L)}-(J\sinh\phi+\delta_L)\varphi(1,x_2,\ldots,x_j,\ldots,x_{M-1},x_M)=0, \tag{C3a}$$

$$J\sum_{j=1}^{M-1}\sum_{\delta=\pm1}\left(1-\delta_{x_j+\delta,x_{j+\delta}}\right)\varphi(x_1,\ldots,x_j+\delta,\ldots,L)e^{-\delta\phi}-\left[E+2J\cosh\phi\left(M-1/2-\sum_{j=1}^{M-1}\delta_{x_j+1,x_{j+1}}\right)\right]\varphi(x_1,x_2,\ldots,L)$$
$$+Je^{\phi}\,\varphi(x_1,\ldots,x_j,\ldots,L-1)+\delta_L\varphi(1,x_1,\ldots,x_j,\ldots,x_{M-1})+(J\sinh\phi-\delta_R)\,\varphi(x_1,\ldots,x_j,\ldots,x_{M-1},L)=0, \tag{C3b}$$

where the term marked with the wavy line comes from the boundary hopping. If we still use the OBC ansatz, the boundary term exponentially grows with system size, which far outweighs the other terms. This is unreasonable because the equation is dominated only by a boundary term no matter how small δ_R is. Therefore, an alternative ansatz should be employed. Suppose the quasimomentum takes a complex value and we perform the substitution $k_j\to k_j+i\phi$. We find that this substitution cancels the exponential divergence in the boundary term. The boundary equation (C3b) gives rise to the relation $\frac{A_{\mathbf{P}}(r_1,r_2,\ldots,-)}{A_{\mathbf{P}}(r_1,r_2,\ldots,+)}\sim e^{-2\phi L}$, which means $\frac{A_{\mathbf{P}}(r_1,r_2,\ldots,-)}{A_{\mathbf{P}}(r_1,r_2,\ldots,+)}\to0$ in the large-L limit. Moreover, when $x_{j+1}=x_j+1$, the contact condition gives

$$\frac{A_{P_1,\ldots,P_j,P_{j+1},\ldots,P_M}(r_1,\ldots,r_j,r_{j+1},\ldots,r_M)}{A_{P_1,\ldots,P_{j+1},P_j,\ldots,P_M}(r_1,\ldots,r_{j+1},r_j,\ldots,r_M)}=-\frac{S(k_{P_{j+1}},k_{P_j})}{S(k_{P_j},k_{P_{j+1}})}. \tag{C4}$$

Combining Eq. (C4) with the condition $\frac{A_{\mathbf{P}}(r_1,r_2,\ldots,-)}{A_{\mathbf{P}}(r_1,r_2,\ldots,+)}\to0$ indicates that all coefficients $A_{\mathbf{P}}(r_1,r_2,\ldots,r_M)$ for any $r_j=-1$ are zero. The vanishing left-moving wave indicates a no-reflecting boundary condition in the thermodynamic limit. As a result, we modify the PBC wave function by a substitution into the PBC wave function $e^{ik_{P_j}x_j}\to\lambda^{\frac{x_j}{L}}e^{ik_{P_j}x_j}$, with $\lambda=\frac{Je^{\phi}}{\delta_R}$, and hence, $\varphi(x_1,x_2,\ldots,x_M)=\sum_{\mathbf{P}}A_{\mathbf{P}}\exp(i\sum_{j=1}^{M}k_{p_j}x_j+x_j\ln\lambda)$. After this substitution, the coefficient δ_L of the term with the wavy line in (C3a) transforms to J_R, which is the same as the boundary hopping in the PBC. In fact, from boundary condition (C3a), using the modified PBC wave function, one can derive PBC-like BAEs,

$$\exp(ik_jL)=(-1)^{M-1}\kappa\prod_{l\neq j}^{M}\frac{\exp[i(k_j+k_l)-2\phi]+1-2\cosh\phi\exp(ik_j-\phi)}{\exp[i(k_j+k_l)-2\phi]+1-2\cosh\phi\exp(ik_l-\phi)}. \tag{C5}$$

We can see clearly that BAEs (C5) are the same as the ones in the PBC case up to the coefficient $\kappa=1-\frac{(J_L-\delta_L)(\frac{J_R}{\delta_R})^{1/L}e^{ik_j}}{J_R}$, which serves as a boundary term. However, the boundary term just produces a $1/L$ correction which vanishes in the large-L limit, which means no LSE exists.

[1] Y. Ashida, Z. Gong, and M. Ueda, Non-Hermitian physics, Adv. Phys. **69**, 249 (2020).

[2] E. J. Bergholtz, J. C. Budich, and F. K. Kunst, Exceptional topology of non-Hermitian systems, Rev. Mod. Phys. **93**, 015005 (2021).

[3] V. Meden, L. Grunwald, and D. M. Kennes, $\mathcal{PT}$-symmetric, non-Hermitian quantum many-body physics–A methodological perspective, Rep. Prog. Phys. **86**, 124501 (2023).

[4] G. Barontini, R. Labouvie, F. Stubenrauch, A. Vogler, V. Guarrera, and H. Ott, Controlling the dynamics of an open many-body quantum system with localized dissipation, Phys. Rev. Lett. **110**, 035302 (2013).

[5] Y. S. Patil, S. Chakram, and M. Vengalattore, Measurement-induced localization of an ultracold lattice gas, Phys. Rev. Lett. **115**, 140402 (2015).

[6] R. Labouvie, B. Santra, S. Heun, and H. Ott, Bistability in a driven-dissipative superfluid, Phys. Rev. Lett. **116**, 235302 (2016).

[7] H. P. Lüschen, P. Bordia, S. S. Hodgman, M. Schreiber, S. Sarkar, A. J. Daley, M. H. Fischer, E. Altman, I. Bloch, and U. Schneider, Signatures of many-body localization in a controlled open quantum system, Phys. Rev. X **7**, 011034 (2017).

[8] T. Tomita, S. Nakajima, Y. Takasu, and Y. Takahashi, Dissipative Bose-Hubbard system with intrinsic two-body loss, Phys. Rev. A **99**, 031601(R) (2019).

[9] R. Bouganne, M. B. Aguilera, A. Ghermaoui, and F. Gerbier, Anomalous decay of coherence in a dissipative many-body system, Nat. Phys. **16**, 21 (2020).

[10] T. Tomita, S. Nakajima, I. Danshita, Y. Takasu, and Y. Takahashi, Observation of the Mott insulator to superfluid crossover of a driven-dissipative Bose-Hubbard system, Sci. Adv. **3**, e1701513 (2017).

[11] K. Sponselee, L. Freystatzky, B. Abeln, M. Diem, B. Hundt, A. Kochanke, T. Ponath, B. Santra, L. Mathey, K. Sengstock, and C. Becker, Dynamics of ultracold quantum gases in the dissipative Fermi–Hubbard model, Quantum Sci. Technol. **4**, 014002 (2018).

[12] Y. Takasu, T. Yagami, Y. Ashida, R. Hamazaki, Y. Kuno, and Y. Takahashi, PT-symmetric non-Hermitian quantum many-body system using ultracold atoms in an optical lattice with controlled dissipation, Prog. Theor. Exp. Phys. **2020**, 12A110 (2020).

[13] B. Yan, S. A. Moses, B. Gadway, J. P. Covey, K. R. Hazzard, A. M. Rey, D. S. Jin, and J. Ye, Observation of dipolar spin-exchange interactions with lattice-confined polar molecules, Nature (London) **501**, 521 (2013).

[14] F. Schäfer, T. Fukuhara, S. Sugawa, Y. Takasu, and Y. Takahashi, Tools for quantum simulation with ultracold atoms in optical lattices, Nat. Rev. Phys. **2**, 411 (2020).

[15] Y. Zhao, Y. Tian, J. Ye, Y. Wu, Z. Zhao, Z. Chi, T. Tian, H. Yao, J. Hu, Y. Chen, and W. Chen, Observation of universal dissipative dynamics in strongly correlated quantum gas, arXiv:2309.10257.

[16] K. Kawabata, Y. Ashida, and M. Ueda, Information retrieval and criticality in parity-time-symmetric systems, Phys. Rev. Lett. **119**, 190401 (2017).

[17] Y. Ashida, S. Furukawa, and M. Ueda, Parity-time-symmetric quantum critical phenomena, Nat. Commun. **8**, 15791 (2017).

[18] L. Pan, S. Chen, and X. Cui, High-order exceptional points in ultracold Bose gases, Phys. Rev. A **99**, 011601(R) (2019).

[19] L. Pan, S. Chen, and X. Cui, Interacting non-Hermitian ultracold atoms in a harmonic trap: Two-body exact solution and a high-order exceptional point, Phys. Rev. A **99**, 063616 (2019).

[20] Z. Zhou and Z. Yu, Interaction effects on the $\mathscr{P}\mathscr{T}$-symmetry-breaking transition in atomic gases, Phys. Rev. A **99**, 043412 (2019).

[21] K. Yamamoto, M. Nakagawa, K. Adachi, K. Takasan, M. Ueda, and N. Kawakami, Theory of non-Hermitian fermionic superfluidity with a complex-valued interaction, Phys. Rev. Lett. **123**, 123601 (2019).

[22] N. Okuma and M. Sato, Topological phase transition driven by infinitesimal instability: Majorana fermions in non-Hermitian spintronics, Phys. Rev. Lett. **123**, 097701 (2019).

[23] L. Zhou and X. Cui, Enhanced fermion pairing and superfluidity by an imaginary magnetic field, iScience **14**, 257 (2019).

[24] L. Pan, X. Chen, Y. Chen, and H. Zhai, Non-Hermitian linear response theory, Nat. Phys. **16**, 767 (2020).

[25] L. Pan, Non-Hermitian linear response theory and its applications, Acta Phys. Sin. **71**, 170305 (2022).

[26] T. Yoshida, K. Kudo, and Y. Hatsugai, Non-Hermitian fractional quantum Hall states, Sci. Rep. **9**, 16895 (2019).

[27] T. Liu, J. J. He, T. Yoshida, Z.-L. Xiang, and F. Nori, Non-Hermitian topological Mott insulators in one-dimensional fermionic superlattices, Phys. Rev. B **102**, 235151 (2020).

[28] Z. H. Xu and S. Chen, Topological Bose-Mott insulators in one-dimensional non-Hermitian superlattices, Phys. Rev. B **102**, 035153 (2020).

[29] K. Kawabata, K. Shiozaki, and S. Ryu, Many-body topology of non-Hermitian systems, Phys. Rev. B **105**, 165137 (2022).

[30] S.-B. Zhang, M. M. Denner, T. Bzdušek, M. A. Sentef, and T. Neupert, Symmetry breaking and spectral structure of the interacting Hatano-Nelson model, Phys. Rev. B **106**, L121102 (2022).

[31] J. Carlström, Correlations in non-Hermitian systems and diagram techniques for the steady state, Phys. Rev. Res. **2**, 013078 (2020).

[32] Z. Cai and T. Barthel, Algebraic versus exponential decoherence in dissipative many-particle systems, Phys. Rev. Lett. **111**, 150403 (2013).

[33] T.-S. Deng, L. Pan, Y. Chen, and H. Zhai, Stability of time-reversal symmetry protected topological phases, Phys. Rev. Lett. **127**, 086801 (2021).

[34] Z. Wang, Q. Li, W. Li, and Z. Cai, Symmetry-protected topological edge modes and emergent partial time-reversal symmetry breaking in open quantum many-body systems, Phys. Rev. Lett. **126**, 237201 (2021).

[35] T.-S. Deng and L. Pan, Fate of symmetry protected coherence in open quantum system, Phys. Rev. B **104**, 094306 (2021).

[36] B. Buča, C. Booker, M. Medenjak, and D. Jaksch, Bethe ansatz approach for dissipation: Exact solutions of quantum many-body dynamics under loss, New J. Phys. **22**, 123040 (2020).

[37] K. Yamamoto, Y. Ashida, and N. Kawakami, Rectification in nonequilibrium steady states of open many-body systems, Phys. Rev. Res. **2**, 043343 (2020).

[38] K. Yamamoto, M. Nakagawa, N. Tsuji, M. Ueda, and N. Kawakami, Collective excitations and nonequilibrium phase transition in dissipative fermionic superfluids, Phys. Rev. Lett. **127**, 055301 (2021).

[39] R. Hanai, A. Edelman, Y. Ohashi, and P. B. Littlewood, Non-Hermitian phase transition from a polariton Bose-Einstein condensate to a photon laser, Phys. Rev. Lett. **122**, 185301 (2019).

[40] K. L. Zhang and Z. Song, Quantum phase transition in a quantum Ising chain at nonzero temperatures, Phys. Rev. Lett. **126**, 116401 (2021).

[41] X. Z. Zhang and Z. Song, Probing the superfluid-insulator phase transition by a non-Hermitian external field, Phys. Rev. B **104**, 094301 (2021).

[42] X. Z. Zhang, L. Jin, and Z. Song, Dynamic magnetization in non-Hermitian quantum spin systems, Phys. Rev. B **101**, 224301 (2020).

[43] K. L. Zhang and Z. Song, Building ground states of the Hubbard model by time-ordered bound-pair injection, Phys. Rev. B **104**, 245140 (2021).

[44] D. Sticlet, B. Dóra, and C. P. Moca, Kubo formula for non-Hermitian systems and tachyon optical conductivity, Phys. Rev. Lett. **128**, 016802 (2022).

[45] B. Dóra, and C. P. Moca, Quantum quench in $\mathscr{P}\mathscr{T}$-symmetric Luttinger liquid, Phys. Rev. Lett. **124**, 136802 (2020).

[46] Á. Bácsi, C. P. Moca, and B. Dóra, Dissipation-induced Luttinger liquid correlations in a one-dimensional Fermi gas, Phys. Rev. Lett. **124**, 136401 (2020).

[47] J.-S. Bernier, R. Tan, C. Guo, C. Kollath, and D. Poletti, Melting of the critical behavior of a Tomonaga-Luttinger liquid under dephasing, Phys. Rev. B **102**, 115156 (2020).

[48] L. Pan, X. Wang, X. Cui, and S. Chen, Interaction-induced dynamical $\mathscr{P}\mathscr{T}$-symmetry breaking in dissipative Fermi-Hubbard models, Phys. Rev. A **102**, 023306 (2020).

[49] X. Z. Zhang and Z. Song, Dynamical preparation of a steady off-diagonal long-range order state in the Hubbard model with a local non-Hermitian impurity, Phys. Rev. B **102**, 174303 (2020).

[50] X. Z. Zhang and Z. Song, η-pairing ground states in the non-Hermitian Hubbard model, Phys. Rev. B **103**, 235153 (2021).

[51] T. Hayata and A. Yamamoto, Non-Hermitian Hubbard model without the sign problem, Phys. Rev. B **104**, 125102 (2021).

[52] K. Yang, S. C. Morampudi, and E. J. Bergholtz, Exceptional spin liquids from couplings to the environment, Phys. Rev. Lett. **126**, 077201 (2021).

[53] X. Cui, Quantum fluctuations on top of a $\mathscr{P}\mathscr{T}$-symmetric Bose-Einstein condensate, Phys. Rev. Res. **4**, 013047 (2022).

[54] M. Nakagawa, N. Kawakami, and M. Ueda, Exact Liouvillian spectrum of a one-dimensional dissipative Hubbard model, Phys. Rev. Lett. **126**, 110404 (2021).

[55] M. Nakagawa, N. Tsuji, N. Kawakami, and M. Ueda, Dynamical sign reversal of magnetic correlations in dissipative Hubbard models, Phys. Rev. Lett. **124**, 147203 (2020).

[56] R. Hamazaki, K. Kawabata, and M. Ueda, Non-Hermitian many-body localization, Phys. Rev. Lett. **123**, 090603 (2019).

[57] L.-J. Zhai, S. Yin, and G.-Y. Huang, Many-body localization in a non-Hermitian quasiperiodic system, Phys. Rev. B **102**, 064206 (2020).

[58] K. Suthar, Y.-C. Wang, Y.-P. Huang, H.-H. Jen, and J.-S. You, Non-Hermitian many-body localization with open boundaries, Phys. Rev. B **106**, 064208 (2022).

[59] C. Ehrhardt and J. Larson, Exploring the impact of fluctuation-induced criticality on non-Hermitian skin effect and quantum sensors, Phys. Rev. Res. **6**, 023135 (2024).

[60] F. Roccati, F. Balducci, R. Shir, and A. Chenu, Diagnosing non-Hermitian many-body localization and quantum chaos via singular value decomposition, Phys. Rev. B **109**, L140201 (2024).

[61] N. Matsumoto, K. Kawabata, Y. Ashida, S. Furukawa, and M. Ueda, Continuous phase transition without gap closing in Non-Hermitian quantum many-body systems, Phys. Rev. Lett. **125**, 260601 (2020).

[62] S. Sarkar, A study of quantum Berezinskii–Kosterlitz–Thouless transition for parity-time symmetric quantum criticality, Sci. Rep. **11**, 5510 (2021).

[63] M. Nakagawa, N. Kawakami, and M. Ueda, Non-Hermitian Kondo effect in ultracold alkaline-earth atoms, Phys. Rev. Lett. **121**, 203001 (2018).

[64] J. A. S. Lourenço, R. L. Eneias, and R. G. Pereira, Kondo effect in a $\mathscr{P}\mathscr{T}$-symmetric non-Hermitian Hamiltonian, Phys. Rev. B **98**, 085126 (2018).

[65] R. Hanai and P. B. Littlewood, Critical fluctuations at a many-body exceptional point, Phys. Rev. Res. **2**, 033018 (2020).

[66] K. Yamamoto, M. Nakagawa, M. Tezuka, M. Ueda, and N. Kawakami, Universal properties of dissipative Tomonaga-Luttinger liquids: Case study of a non-Hermitian XXZ spin chain, Phys. Rev. B **105**, 205125 (2022).

[67] Y.-N. Zhou, L. Mao, and H. Zhai, Rényi entropy dynamics and Lindblad spectrum for open quantum systems, Phys. Rev. Res. **3**, 043060 (2021).

[68] P. Zhang, S.-K. Jian, C. Liu, and X. Chen, Emergent replica conformal symmetry in Non-Hermitian SYK_2 chains, Quantum **5**, 579 (2021).

[69] L. Sá, P. Ribeiro, and T. Prosen, Complex spacing ratios: A signature of dissipative quantum chaos, Phys. Rev. X **10**, 021019 (2020).

[70] J. Li, T. Prosen, and A. Chan, Spectral statistics of non-Hermitian matrices and dissipative quantum chaos, Phys. Rev. Lett. **127**, 170602 (2021).

[71] G. Sun, J.-C. Tang, and S.-P. Kou, Biorthogonal quantum criticality in non-Hermitian many-body systems, Front. Phys. **17**, 33502 (2022).

[72] S. Mu, C. H. Lee, L. Li, and J. Gong, Emergent Fermi surface in a many-body non-Hermitian fermionic chain, Phys. Rev. B **102**, 081115(R) (2020).

[73] F. Qin, R. Shen, and C. H. Lee, Non-Hermitian squeezed polarons, Phys. Rev. A **107**, L010202 (2023).

[74] P.-Y. Chang, J.-S. You, X. Wen, and S. Ryu, Entanglement spectrum and entropy in topological non-Hermitian systems and nonunitary conformal field theory, Phys. Rev. Res. **2**, 033069 (2020).

[75] T. Sanno, M. G. Yamada, T. Mizushima, and S. Fujimoto, Engineering Yang-Lee anyons via Majorana bound states, Phys. Rev. B **106**, 174517 (2022).

[76] S. Longhi, Phase transitions and bunching of correlated particles in a non-Hermitian quasicrystal, Phys. Rev. B **108**, 075121 (2023).

[77] T. Mori, Liouvillian-gap analysis of open quantum many-body systems in the weak dissipation limit, Phys. Rev. B **109**, 064311 (2024).

[78] C.-Z. Lu, X. Deng, S.-P. Kou, and G. Sun, Unconventional many-body phase transitions in a non-Hermitian Ising chain, arXiv:2311.11251.

[79] S. Yao, and Z. Wang, Edge states and topological invariants of non-Hermitian systems, Phys. Rev. Lett. **121**, 086803 (2018).
[80] S. Yao, F. Song, and Z. Wang, Non-Hermitian Chern bands, Phys. Rev. Lett. **121**, 136802 (2018).
[81] F. K. Kunst, E. Edvardsson, J. C. Budich, and E. J. Bergholtz, Biorthogonal bulk-boundary correspondence in non-Hermitian systems, Phys. Rev. Lett. **121**, 026808 (2018).
[82] F. Song, S. Yao, and Z. Wang, Non-Hermitian skin effect and chiral damping in open quantum systems, Phys. Rev. Lett. **123**, 170401 (2019).
[83] F. Song, S. Yao, and Z. Wang, Non-Hermitian topological invariants in real space, Phys. Rev. Lett. **123**, 246801 (2019).
[84] H. Jiang, L.-J. Lang, C. Yang, S.-L. Zhu, and S. Chen, Interplay of non-Hermitian skin effects and Anderson localization in nonreciprocal quasiperiodic lattices, Phys. Rev. B **100**, 054301 (2019).
[85] C.-X. Guo, C.-H. Liu, X.-M. Zhao, Y. Liu, and S. Chen, Phys. Rev. Lett. **127**, 116801 (2021).
[86] L. Jin and Z. Song, Bulk-boundary correspondence in a non-Hermitian system in one dimension with chiral inversion symmetry, Phys. Rev. B **99**, 081103(R) (2019).
[87] D. S. Borgnia, A. J. Kruchkov, and R.-J. Slager, Non-Hermitian boundary modes and topology, Phys. Rev. Lett. **124**, 056802 (2020).
[88] S. Longhi, Probing non-Hermitian skin effect and non-Bloch phase transitions, Phys. Rev. Res. **1**, 023013 (2019).
[89] K. Zhang, Z. Yang, and C. Fang, Correspondence between winding numbers and skin modes in non-Hermitian systems, Phys. Rev. Lett. **125**, 126402 (2020).
[90] C. H. Lee, L. Li, and J. Gong, Hybrid higher-order skin-topological modes in nonreciprocal systems, Phys. Rev. Lett. **123**, 016805 (2019).
[91] L. Li, C. H. Lee, and J. Gong, Topological switch for Non-Hermitian skin effect in cold-atom systems with loss, Phys. Rev. Lett. **124**, 250402 (2020).
[92] L. Li, C. H. Lee, S. Mu, and J. Gong, Critical non-Hermitian skin effect, Nat. Commun. **11**, 5491 (2020).
[93] C.-H. Liu, K. Zhang, Z. Yang, and S. Chen, Phys. Rev. Res. **2**, 043167 (2020).
[94] J. C. Budich and E. J. Bergholtz, Non-Hermitian topological sensors, Phys. Rev. Lett. **125**, 180403 (2020).
[95] Z. Yang, K. Zhang, C. Fang, and J. Hu, Non-Hermitian bulk-boundary correspondence and auxiliary generalized Brillouin zone theory, Phys. Rev. Lett. **125**, 226402 (2020).
[96] T. Yoshida, T. Mizoguchi, and Y. Hatsugai, Mirror skin effect and its electric circuit simulation, Phys. Rev. Res. **2**, 022062(R) (2020).
[97] Y. Yi and Z. Yang, Non-Hermitian skin modes induced by on-site dissipations and chiral tunneling effect, Phys. Rev. Lett. **125**, 186802 (2020).
[98] N. Okuma, K. Kawabata, K. Shiozaki, and M. Sato, Topological origin of Non-Hermitian skin effects, Phys. Rev. Lett. **124**, 086801 (2020).
[99] S. Longhi, Non-Bloch-band collapse and chiral Zener tunneling, Phys. Rev. Lett. **124**, 066602 (2020).
[100] Z. Zhou and Z. Yu, Non-Hermitian skin effect in quadratic Lindbladian systems: An adjoint fermion approach, Phys. Rev. A **106**, 032216 (2022).
[101] S. Guo, C. Dong, F. Zhang, J. Hu, and Z. Yang, Theoretical prediction of a non-Hermitian skin effect in ultracold-atom systems, Phys. Rev. A **106**, L061302 (2022).
[102] L. Zhou, H. Li, W. Yi, and X. Cui, Engineering non-Hermitian skin effect with band topology in ultracold gases, Commun. Phys **5**, 252 (2022).
[103] K. Zhang, Z. Yang, and C. Fang, Universal non-Hermitian skin effect in two and higher dimensions, Nat. Commun. **13**, 2496 (2022).
[104] Y. Peng, J. Jie, D. Yu, and Y. Wang, Manipulating the non-Hermitian skin effect via electric fields, Phys. Rev. B **106**, L161402 (2022).
[105] X. Zhang, T. Zhang, M.-H. Lu, and Y.-F. Chen, A review on non-Hermitian skin effect, Adv. Phys. X **7**, 2109431 (2022).
[106] Y.-P. Wang, C. Fang, and J. Ren, Absence of measurement-induced entanglement transition due to feedback-induced skin effect, Phys. Rev. B **110**, 035113 (2024).
[107] X. Feng, S. Liu, S. Chen, and W. Guo, Absence of logarithmic and algebraic scaling entanglement phases due to the skin effect, Phys. Rev. B **107**, 094309 (2023).
[108] T. Helbig, T. Hofmann, S. Imhof, M. Abdelghany, T. Kiessling, L. W. Molenkamp, C. H. Lee, A. Szameit, M. Greiter, and R. Thomale, Generalized bulk–boundary correspondence in non-Hermitian topolectrical circuits, Nat. Phys. **16**, 747 (2020).
[109] T. Hofmann, T. Helbig, F. Schindler, N. Salgo, M. Brzezinska, M. Greiter, T. Kiessling, D. Wolf, A. Vollhardt, A. Kabasi, C. H. Lee, A. Bilusic, R. Thomale, and T. Neupert, Reciprocal skin effect and its realization in a topolectrical circuit, Phys. Rev. Res. **2**, 023265 (2020).
[110] L. Xiao, T. Deng, K. Wang, G. Zhu, Z. Wang, W. Yi, and P. Xue, Non-Hermitian bulk–boundary correspondence in quantum dynamics, Nat. Phys. **16**, 761 (2020).
[111] A. Ghatak, M. Brandenbourger, J. van Wezel, and C. Coulais, Observation of non-Hermitian topology and its bulk–edge correspondence in an active mechanical metamaterial, Proc. Natl. Acad. Sci. USA **117**, 29561 (2020).
[112] S. Weidemann, M. Kremer, T. Helbig, T. Hofmann, A. Stegmaier, M. Greiter, R. Thomale, and A. Szameit, Topological funneling of light, Science **368**, 311 (2020).
[113] D. Zou, T. Chen, W. He, J. Bao, C. H. Lee, H. Sun, and X. Zhang, Observation of hybrid higher-order skin-topological effect in non-Hermitian topolectrical circuits, Nat. Commun. **12**, 7201 (2021).
[114] L. Zhang, Y. Yang, Y. Ge, Y.-J. Guan, Q. Chen, Q. Yan, F. Chen, R. Xi, Y. Li, D. Jia, S.-Q. Yuan, H.-X. Sun, H. Chen, and B. Zhang, Acoustic non-Hermitian skin effect from twisted winding topology, Nat. Commun. **12**, 6297 (2021).
[115] X. Zhang, Y. Tian, J.-H. Jiang, M.-H. Lu, and Y.-F. Chen, Observation of higher-order non-Hermitian skin effect, Nat. Commun. **12**, 5377 (2021).
[116] Q. Liang, D. Xie, Z. Dong, H. Li, H. Li, B. Gadway, W. Yi, and B. Yan, Dynamic signatures of non-Hermitian skin effect and topology in ultracold atoms, Phys. Rev. Lett. **129**, 070401 (2022).
[117] T. Haga, M. Nakagawa, R. Hamazaki, and M. Ueda, Liouvillian skin effect: Slowing down of relaxation processes without gap closing, Phys. Rev. Lett. **127**, 070402 (2021).

[118] C. H. Lee, Many-body topological and skin states without open boundaries, Phys. Rev. B **104**, 195102 (2021).
[119] R. Shen and C. H. Lee, Non-Hermitian skin clusters from strong interactions, Commun. Phys. **5**, 238 (2022).
[120] D.-W. Zhang, Y.-L. Chen, G.-Q. Zhang, L.-J. Lang, Z. Li, and S.-L. Zhu, Skin superfluid, topological Mott insulators, and asymmetric dynamics in an interacting non-Hermitian Aubry-André-Harper model, Phys. Rev. B **101**, 235150 (2020).
[121] Z. Wang, L.-J. Lang, and L. He, Emergent Mott insulators and non-Hermitian conservation laws in an interacting bosonic chain with noninteger filling and nonreciprocal hopping, Phys. Rev. B **105**, 054315 (2022).
[122] N. Okuma and M. Sato, Non-Hermitian skin effects in Hermitian correlated or disordered systems: Quantities sensitive or insensitive to boundary effects and pseudo-quantum-number, Phys. Rev. Lett. **126**, 176601 (2021).
[123] T. Yoshida, Real-space dynamical mean field theory study of non-Hermitian skin effect for correlated, systems: Analysis based on pseudospectrum, Phys. Rev. B **103**, 125145 (2021).
[124] F. Alsallom, L. Herviou, O. V. Yazyev, and M. Brzezińska, Fate of the non-Hermitian skin effect in many-body fermionic systems, Phys. Rev. Res. **4**, 033122 (2022).
[125] W. N. Faugno and T. Ozawa, Interaction-induced Non-Hermitian topological phases from a dynamical gauge field, Phys. Rev. Lett. **129**, 180401 (2022).
[126] T. Yoshida and Y. Hatsugai, Reduction of one-dimensional non-Hermitian point-gap topology by interactions, Phys. Rev. B **106**, 205147 (2022).
[127] H. Li, H. Wu, W. Zheng, and W. Yi, Many-body non-Hermitian skin effect under dynamic gauge coupling, Phys. Rev. Res. **5**, 033173 (2023).
[128] Y.-C. Wang, K. Suthar, H. H. Jen, Y.-T. Hsu, and J.-S. You, Non-Hermitian skin effects on thermal and many-body localized phases, Phys. Rev. B **107**, L220205 (2023).
[129] S.-K. Jian, Z.-C. Yang, Z. Bi, and X. Chen, Yang-Lee edge singularity triggered entanglement transition, Phys. Rev. B **104**, L161107 (2021).
[130] C.-Z. Lu and G. Sun, Many-body entanglement and spectral clusters in the extended hard-core bosonic Hatano-Nelson model, Phys. Rev. A **109**, 042208 (2024).
[131] Z.-C. Liu, K. Li, and Y. Xu, Dynamical phase transition due to feedback-induced skin effect, arXiv:2311.16541.
[132] L. Mao, Y. Hao, and L. Pan, Non-Hermitian skin effect in a one-dimensional interacting Bose gas, Phys. Rev. A **107**, 043315 (2023).
[133] K. Cao, Q. Du, and S.-P. Kou, Many-body non-Hermitian skin effect at finite temperatures, Phys. Rev. B **108**, 165420 (2023).
[134] F. Yang, Q.-D. Jiang, and E. J. Bergholtz, Liouvillian skin effect in an exactly solvable model, Phys. Rev. Res. **4**, 023160 (2022).
[135] X. Feng and S. Chen, Boundary-sensitive Lindbladians and relaxation dynamics, Phys. Rev. B **109**, 014313 (2024).
[136] S. Hamanaka, K. Yamamoto, and T. Yoshida, Interaction-induced Liouvillian skin effect in a fermionic chain with a two-body loss, Phys. Rev. B **108**, 155114 (2023).
[137] Z. Wang, Y. Lu, Y. Peng, R. Qi, Y. Wang, and J. Jie, Accelerating relaxation dynamics in open quantum systems with Liouvillian skin effect, Phys. Rev. B **108**, 054313 (2023).
[138] M. V. Medvedyeva, F. H. L. Essler, and T. Prosen, Exact Bethe ansatz spectrum of a tight-binding chain with dephasing noise, Phys. Rev. Lett. **117**, 137202 (2016).
[139] G. Akemann, M. Kieburg, A. Mielke, and T. Prosen, Universal signature from integrability to chaos in dissipative open quantum systems, Phys. Rev. Lett. **123**, 254101 (2019).
[140] F. H. L. Essler and L. Piroli, Integrability of one-dimensional Lindbladians from operator-space fragmentation, Phys. Rev. E **102**, 062210 (2020).
[141] A. A. Ziolkowska and F. Essler, Yang-Baxter integrable Lindblad equations, SciPost Phys. **8**, 044 (2020).
[142] M. de Leeuw, C. Paletta, and B. Pozsgay, Constructing integrable Lindblad superoperators, Phys. Rev. Lett. **126**, 240403 (2021).
[143] V. Popkov and C. Presilla, Full pectrum of the Liouvillian of open dissipative quantum systems in the Zeno limit, Phys. Rev. Lett. **126**, 190402 (2021).
[144] P. W. Claeys and A. Lamacraft, Dissipative dynamics in open XXZ Richardson-Gaudin models, Phys. Rev. Res. **4**, 013033 (2022).
[145] L. Su and I. Martin, Integrable nonunitary quantum circuits, Phys. Rev. B **106**, 134312 (2022).
[146] C. P. Moca, M. A. Werner, Ö. Legeza, T. Prosen, M. Kormos, and G. Zaránd, Simulating Lindbladian evolution with non-Abelian symmetries: Ballistic front propagation in the SU(2) Hubbard model with a localized loss, Phys. Rev. B **105**, 195144 (2022).
[147] L. Sá, P. Ribeiro, and T. Prosen, Lindbladian dissipation of strongly-correlated quantum matter, Phys. Rev. Res. **4**, L022068 (2022).
[148] H.-R. Wang, B. Li, F. Song, and Z. Wang, Scale-free non-Hermitian skin effect in a boundary-dissipated spin chain, SciPost Phys. **15**, 191 (2023).
[149] M. Zheng, Y. Qiao, Y. Wang, J. Cao, and S. Chen, Exact Solution of the Bose-Hubbard model with unidirectional hopping, Phys. Rev. Lett. **132**, 086502 (2024).
[150] G. Lindblad, On the generators of quantum dynamical semigroups, Commun. Math. Phys. **119**, 48 (1976).
[151] V. Gorini, A. Kossakowski, and E. C. Sudarsahan, Completely positive dynamical semigroups of N-level systems, J. Math. Phys. **17**, 821 (1976).
[152] M.-D. Choi, Completely positive linear maps on complex matrices, Linear Algebra Its Appl. **10**, 285 (1975).
[153] A. Jamiołkowski, Linear transformations which preserve trace and positive semidefiniteness of operators, Rep. Math. Phys. **3**, 275 (1972).
[154] N. Hatano and D. R. Nelson, Localization transitions in non-Hermitian quantum mechanics, Phys. Rev. Lett. **77**, 570 (1996).
[155] G. Albertini, S. R. Dahmen, and B. Wehefritz, Phase diagram of the non-Hermitian asymmetric XXZ spin chain, J. Phys. A **29**, L369 (1996).
[156] T. Fukui and N. Kawakami, Breakdown of the Mott insulator: Exact solution of an asymmetric Hubbard model, Phys. Rev. B **58**, 16051 (1998).